



Published in final edited form as:

*J Magn Reson.* 2009 September ; 200(1): 74–80. doi:10.1016/j.jmr.2009.06.004.

## A strip-shield improves the efficiency of a solenoid coil in probes for high field solid-state NMR of lossy biological samples

Chin H. Wu, Christopher V. Grant, Gabriel A. Cook, Sang Ho Park, and Stanley J. Opella\*  
Department of Chemistry and Biochemistry, 9500 Gilman Drive, University of California, San Diego, La Jolla, CA 92093-0307

### Abstract

A strip-shield inserted between a high inductance double-tuned solenoid coil and the glass tube containing the sample improves the efficiency of probes used for high-field solid-state NMR experiments on lossy aqueous samples of proteins and other biopolymers. A strip-shield is a coil liner consisting of thin copper strips layered on a PTFE (polytetrafluoroethylene) insulator. With lossy samples, the shift in tuning frequency is smaller, the reduction in  $Q$ , and RF-induced heating are all significantly reduced when the strip-shield is present. The performance of 800 MHz  $^1\text{H}/^{15}\text{N}$  and  $^1\text{H}/^{13}\text{C}$  double-resonance probes is demonstrated on aqueous samples of membrane proteins in phospholipid bilayers.

### Keywords

Faraday shield; solenoid coil; double-resonance; membrane proteins

### Introduction

Optimal resolution and sensitivity in solid-state NMR experiments on proteins and other biopolymers are obtained at high magnetic fields. However, a lossy aqueous sample impairs the performance of a typical solenoid-coil solid-state NMR probe in several ways. These effects are strongest at frequencies  $>700$  MHz, but can also have an impact on the performance at lower frequencies. Upon insertion of a lossy sample into a tuned coil, the most noticeable effect is a large change in the center frequency of the circuit. While tuning the probe for lossy samples rather than an empty coil can compensate for this, it limits the ability to switch between lossy and non-lossy samples to tune and set up the spectrometer system for complex experiments. Alternatively, increasing the tuning range to accommodate both lossy and non-lossy samples often results in unstable tuning. The  $Q$  of the circuit is lowered by the lossy sample, decreasing the efficiency of the probe. A complicating factor is that the individual high ( $^1\text{H}$ ) and low ( $^{15}\text{N}$ ,  $^{13}\text{C}$ ) frequency channels in double- or triple- tuned probes are differentially affected, with a stronger effect on the high frequency channel. The severe heating of lossy samples by high frequency RF irradiation has been addressed in a number of recently described probes principally through the use of alternative coil geometries [1;2;3]. However, a conventional solenoid coil has excellent performance characteristics for both the high and low frequency

© 2009 Elsevier Inc. All rights reserved.

\*Corresponding Author: [sopella@ucsd.edu](mailto:sopella@ucsd.edu).

**Publisher's Disclaimer:** This is a PDF file of an unedited manuscript that has been accepted for publication. As a service to our customers we are providing this early version of the manuscript. The manuscript will undergo copyediting, typesetting, and review of the resulting proof before it is published in its final citable form. Please note that during the production process errors may be discovered which could affect the content, and all legal disclaimers that apply to the journal pertain.

channels; its only limitations arise from the deleterious effects of lossy samples. The strip-shield described in this article provides a mechanism for retaining the favorable characteristics of solenoid coils in probes used for high-field solid-state NMR on lossy samples.

In probes used for double- or triple- resonance experiments, the design can be categorized as either multiple-tuned single-coil or cross-coil, both of which are operated in a “single coil” in the traditional sense that the same coil is used for both the transmission and receiving of radiofrequencies in the course of the experiments. A conventional solenoid coil has the best performance for  $^{13}\text{C}$  and  $^{15}\text{N}$  for both lossy and non-lossy samples because their resonance frequencies are <250 MHz at currently available field strengths; however, for lossy samples it has severe limitations at  $^1\text{H}$  frequencies >700 MHz. Balancing the RF circuit [4] reduces the RF-induced sample heating, but the effect is still too great for many biological samples. Scroll coil [5] and low-inductance loop gap resonators [6] effectively combat RF-induced sample heating; however, in a multiple-tuned single-coil configuration, they have poor overall performance at lower frequencies, especially for  $^{15}\text{N}$ . Although we have found the scroll coil is ideally suited for  $^1\text{H}/^{31}\text{P}$  double-resonance applications because of the relatively high resonance frequency for  $^{31}\text{P}$ , the principal applications are to  $^{13}\text{C}$  and  $^{15}\text{N}$ , and we have been unable to construct a scroll coil probe with sufficient performance for double- or triple-resonance experiments on stationary samples at high fields. Cross-coil designs have been proposed that utilize a low-inductance loop gap resonator on the high frequency channel and achieve high RF power efficiency by using high-inductance solenoid coil at low frequency channels [3;7]. Although the coils are arranged to be orthogonal by the mechanical design, they still require considerable effort to minimize interactions because of their close proximity. A further complication comes from the inner coil having a better filling factor and consequently better performance than the outer coil.

As implied by this brief overview of competing designs, there is not going to be single “best choice” coil arrangement, if for no other reason than that there are now a wide variety of samples being studied by solid-state NMR, including protein crystals with varying degrees of hydration, phospholipid bilayers on glass plates, magnetically-aligned bilayers (bicelles) in aqueous solution, and frozen solutions of membrane proteins, fibrils, etc. The effects of lossy samples on the coils depend on the inductance of the coil, the size of the samples, and the frequency. Most cross-coil designs use a solenoid coil for the low frequency channels, and RF heating is usually ignored. For typical bicelle samples, the Q reduction of a solenoid coil becomes larger as the volume of the samples or the inductance of the coil increases. At frequencies as low as 71 MHz, the  $^{15}\text{N}$  resonance frequency in a 17.5 Tesla magnet, with a high inductance coil, such as a 6-turn 5 mm ID (inner diameter) 10 mm long solenoid, a bicelle sample lowers the Q by about 10%. As the resonance frequency increases, for example at higher fields or for  $^{13}\text{C}$  channels, the Q is reduced even more dramatically. This is in addition to the primary effects on the high frequency  $^1\text{H}$  channel. Therefore, we sought a probe design that would reduce the E-field for all channels, especially  $^{13}\text{C}$ , in addition to  $^1\text{H}$ . Previously, an outer solenoid coil and an inner low-inductance loop gap resonator have shown promise of reducing the E-field on all channels [8], and others have suggested using a Faraday shield inside a solenoid coil [2;6]. Here we describe a design that utilizes an outer multiple tuned solenoid coil in combination with an inner shield inserted between the coil and the sample. The shield consists of thin copper strips that are not connected to each other or to ground. Each rectangular copper strip is approximately the same length as the solenoid coil. The sum of the widths of all of the strips is less than half the circumference of the solenoid coil. The strips are arranged with their long axis parallel to the axis of the solenoid coil and are equally spaced along the circumference. The copper strips and the outer solenoid coil are separated by a thin sheet of dielectric material, e.g. PTFE (polytetrafluoroethylene), to prevent arcing between the coil and the copper strips. Since the strips and the dielectric material reduce the filling factor of the coil, it is incumbent to utilize the thinnest shield that is practicable. The copper strips are very thin

(0.002–0.003 inch) and require support by the PTFE sheet. With the current implementation, in order to accept a 5 mm OD (outer diameter) sample tube, the ID (inner diameter) of the solenoid coil is expanded slightly, to 5.6 mm, in order to have sufficient clearance for the copper strip-containing shield.

Following standard practice, the single solenoid coil can be double or triple tuned [9]. Unlike many cross-coil designs [3;7] where the electric field reduction only affects the  $^1\text{H}$  channel, all channels benefit in this design, and at the  $^{13}\text{C}$  resonance frequency, the RF heating effect is reduced and the probe efficiency is improved.

## Experimental

### Samples

The 63-residue membrane protein p7 of HCV (hepatitis C virus) was uniformly  $^{15}\text{N}$  labeled by expression in *E. coli* containing the requisite gene and grown on M9 minimal media with  $^{15}\text{N}$  ammonium sulfate (Cambridge Isotope Laboratories ([www.isotope.com](http://www.isotope.com))) as the sole nitrogen source. The  $^{13}\text{C}$ -labeled sample of the membrane bound form of Pf1 coat protein was obtained by supplementing the growth media for *P. aeruginosa* with [2- $^{13}\text{C}$ ]-glycerol (Cambridge Isotope Laboratories) as the sole carbon source [10]. The protein-containing bicelle samples for the NMR experiments were prepared as previously described [11]. Approximately 3 mg of lyophilized protein was dissolved in 9.5 mg of the short chain lipid, 6-O-PC, in 200  $\mu\text{l}$  of water. The pH of the p7 sample was adjusted to 4.0, and that of the Pf1 coat protein sample to 6.9. The samples were vortexed, and the resulting clear solution was added to 45.6 mg of 14-O-PC. The final molar ratio of long chain (C14) to short chain (C6) lipids,  $q$ , was 3.2, and the total lipid concentration was 28% (w/v). The resulting samples have very high dielectric constants and are very lossy.

### Strip-shield

Because the strip-shield resides between the solenoid coil and the sample, the space that it occupies reduces the filling factor of the coil. On the one hand, minimizing the thickness of the shield improves the filling factor by enabling the use of a smaller diameter solenoid coil. On the other, the dielectric material in the shield must be thick enough to prevent arcing between the solenoid coil and the copper strips in the shield. The probes described in this article accommodate a 5 mm OD glass tube that contains about 150  $\mu\text{l}$  total volume of sample.

The construction of the strip-shield is illustrated with the photographs in Figure 1. Shown in Figure 1A is a 3/4 inch wide by 41/64 inch long rectangular sheet cut from a large panel containing many of these units. The sheet is made from OFHC (oxygen-free high conductivity) electroplated onto PTFE. It contains 16 copper strips, each of which is 14/32 inch long and 1/64 inch wide. With the copper strips on the outside, the rectangular sheet is rolled so that the ends meet in the middle as shown in Figure 1B. The two ends are placed as close as possible in order to form a uniform shield. The copper is cleaned and dried before taping in order to prevent corrosion. As shown in Figure 1C, PTFE tape (part number 76475A13 from McMaster-Carr ([www.mcmaster.com](http://www.mcmaster.com))) that is 3/4 inch wide and 0.0035 inch thick is applied to one side. Then the shield is tightly wrapped around a 5 mm ID solid rod that acts as a former (Figure 1D), and wrapped with two additional layers of PTFE tape. Excess PTFE on both sides of the copper shield is trimmed with a sharp blade, resulting in a compact, stable strip-shield (Figure 1E), which can be easily slid off the tapered former. The OD of the completed strip-shield is approximately 5.6 mm. The strip-shield is inserted into a 5.6 mm ID solenoid coil (Figure 1F and 1G). A tight friction fit of the strip-shield in the solenoid coil is crucial for stability. Additional layers of PTFE tape can be wrapped around the strip-shield prior to insertion in order to adjust its thickness if necessary. The position of the strip-shield relative to the solenoid

coil is an important factor that is optimized empirically. The  $^1\text{H}$  resonance frequency is monitored using a network analyzer, and the position of the strip-shield is adjusted manually until the lowest  $^1\text{H}$  resonance frequency is observed.

The strips of copper were electroplated onto PTFE according to patterns we designed and submitted to Polyflon Company ([www.polyflon.com](http://www.polyflon.com)) as a custom order to use in their proprietary process. A convenient size for each manufactured panel is 9 inch by 9 inch. With each strip-shield unit having dimensions 3/4 inch by 3/4 inch, 144 strip-shields can be cut out of each panel. The PTFE sheet is 0.002 inch thick, and 0.0014 inch thick OFHC is plated onto it. A wide range of patterns and dimensions were examined. In the selected configuration, the copper strips are equally spaced along the length of the PTFE, and the length of 41/64 inch was chosen principally to create a tight fit for the 5 mm sample tubes. Electroplating copper onto flexible material is a common process in the PCB (printed circuit board) manufacturing industry. It is feasible to use dielectric materials other than PTFE as long as they have good high frequency RF properties. For example, a popular material in flexible PCB manufacturing is polyimide, Kapton ([www.dupont.com](http://www.dupont.com)), which has a high breakdown voltage and can be considered as an alternative dielectric material in situations where  $^{19}\text{F}$  signals from PTFE interfere with experiments. Polyimide tape is also available from many distributors as an off-the-shelf component.

As part of the development process, we also made strip-shields without electroplating the copper onto PTFE using up to 10 copper strips with each strip 1/32 inch wide and Teflon tape (part number 76475A13 from McMaster-Carr) that has a silicon based adhesive hold the copper strips in place; this tape has a proven dielectric strength that can withstand high electric voltage without breakdown. The copper strips were cut out of a sheet of very thin (0.002 in) copper foil (part number 9053K312 from McMaster-Carr), with a sharp blade. The Teflon tape was placed on a flat surface with its adhesive side facing up, and the copper strips were glued onto the Teflon tape. Since the tape is translucent, a ruler placed underneath served to guide the placement of the copper strips. Finally, the copper strips were sandwiched between two layers of Teflon tape and used as illustrated in Figure 1.

### Double-resonance probe construction

Because the probes are used for direct detection of  $^{13}\text{C}$  or  $^{15}\text{N}$  signals, the inductance of the solenoid is made to be as high as possible to optimize the low frequency performance. At 800 MHz with a 5.6 mm ID solenoid coil, we found the performance of the low frequency channel to be only marginally better in a 7-turn compared to a 6-turn coil, however, the performance of the high frequency channel is substantially worse in a 7-turn coil. Therefore, we elected to use 6-turn 5.6 mm ID coils in the probes. The 10 mm long 6-turn coil made of #18 gauge wire has unequal spacing to improve RF homogeneity [12]. With a pick-up coil and network analyzer, we measure the self-resonance frequency of the coil to be 736 MHz without the shield and 537 MHz with the shield inserted. A self-resonance frequency lower than the  $^1\text{H}$  resonance frequency may compromise the  $^1\text{H}$  channel performance somewhat.

In this article, we demonstrate the performance of  $^1\text{H}/^{13}\text{C}$  and  $^1\text{H}/^{15}\text{N}$  double-resonance probes constructed for a standard bore magnet with a field strength corresponding to a  $^1\text{H}$  resonance frequency of 801 MHz, a  $^{13}\text{C}$  resonance frequency of 202 MHz, and a  $^{15}\text{N}$  resonance frequency of 81 MHz with lossy membrane protein samples. By using a custom-made set of “thin” room temperature shims with an ID of 48 mm, the OD of the probe bodies is 48 mm. Annotated photographs of the 800 MHz strip-shield  $^1\text{H}/^{15}\text{N}$  double-resonance probe are shown in Figure 2. The probe cap and outer body have been removed to expose the electrical components. Figure 3 depicts the modified Cross-Waugh circuit diagrams [13] employed in the  $^1\text{H}/^{15}\text{N}$  (Figure 3A) and  $^1\text{H}/^{13}\text{C}$  (Figure 3B) double-resonance probes. The nominal values of the fixed capacitors and the length of L1 are listed in Table 1. The electrical components, including fixed

and variable capacitors and inductors are distributed among three ground planes, which are strongly coupled both mechanically and electrically via the three custom-made, all-threaded brass rods with off-the-shelf M3.5 nuts and washers. By using all-threaded rods, the vertical spacings of the ground planes can be finely adjusted during the assembly process. The probe cap (not shown) fits over the top of the assembly; it is constructed of brass and then gold-plated to prevent oxidation. The probe cap serves as a common ground for all three planes through electrical contacts provided by “gold fingers” (Bruker BioSpin Corporation (www.bruker-biospin.com)), throughout the probe, protects all of the components during handling, and functions as the RF shield. In our experience, the vast majority of instabilities, inefficiencies, and breakdowns result from grounding problems, which are largely eliminated through the combination of close mechanical tolerances and the fine adjustment of the threaded assemblies.

As illustrated in Figure 2 and Figure 3, the electrical components for the  $^1\text{H}$  channel, including the variable capacitors C2 and C3, the fixed capacitors C1 and C4, and the quarter-wavelength coaxial stub L1, are located on the middle ground plane. The tuning components for the  $^{15}\text{N}$  channel, including the variable capacitors C6 and C7 and the fixed capacitors C5 and C8, are located on the bottom ground plane, as are the inductor L2 and the fixed capacitor C9, which form the  $^1\text{H}$  frequency trap. The inductor L3 and the fixed capacitor C11, also tuned to  $^1\text{H}$  frequency, constitute the  $^1\text{H}$  frequency trap in the  $^1\text{H}/^{13}\text{C}$  probe. The four variable capacitors (part number NMNT10-6ENL from Voltronics Corporation (www.voltronicscorp.com)) are screwed into the two lower ground planes, which are made of brass and are silver-plated to prevent oxidation. The fixed capacitors are from American Technical Ceramics Corporation (www.atceramics.com); both 700E and 700C series capacitors are used, depending upon the local space constraints and specific power handling requirements of the circuit. The 700 series capacitors were chosen over the 100 series capacitors because their capacitance values change less in response to heating, which can result from intense RF irradiations. The inductor L1 is a shorted 0.325 inch OD length of semi-rigid coaxial cable (part number UT-325C from Micro-Coax (www.micro-coax.com)). L1 is socketed and can be replaced without desoldering from the ground plane. Both transmission lines, T1 and T2, are semi-rigid coaxial cable with 0.141 inch OD from Micro-Coax, and they are also attached to the ground planes through sockets for ease of replacement.

## Results

In “single coil” probes, which use the same coil for receiving and transmitting, the detection sensitivity can be estimated from the transmitter efficiency based on the reciprocity theorem [14].

The RF field strength,  $B_1$ , is given by [15]:

$$B_1 \propto \sqrt{(PQ/Vf)}$$

Where P is the transmitter power in watts, Q is the probe quality factor, f is the resonance frequency in MHz and V is the coil volume. The probe power efficiency ( $\eta$ ) is defined by [8]:

$$\eta = B_1^2/P \propto Q/Vf$$

Since Q can be measured directly on the bench using a network analyzer, it provides a convenient way to evaluate the probe power efficiency. Table 2 lists the probe Q and the probe

power efficiency with different samples in the coil, with and without the strip-shield present. The  $^1\text{H}$  channel results are measured for the  $^1\text{H}/^{15}\text{N}$  double-resonance probe. The power efficiency is plotted as a function of probe Q and the results are fit to a linear relationship in Figure 4. The slopes are  $0.24 \pm 0.02 \text{ kHz}^2/\text{watt}$ ,  $0.251 \pm 0.004 \text{ kHz}^2/\text{watt}$ ,  $0.066 \pm 0.002 \text{ kHz}^2/\text{watt}$  for the  $^1\text{H}$ ,  $^{13}\text{C}$ , and  $^{15}\text{N}$  channels, respectively.

The strip-shield improves the RF homogeneity of the coil especially for large lossy samples that occupy the entire volume. A  $^1\text{H}$  nutation plot for the water resonance of a typical bicelle sample is presented in Figure 5. The intensity after two full nutations ( $I_{810}$ ) is 88% of the maximum signal intensity ( $I_{810}/I_{90} = 88\%$ ).

The probe Q was measured with a HP 8752A Network analyzer. Calibrating with a HP 85032B calibration kit eliminates the effect of loss from the cable connecting the network analyzer to the probe. The samples are  $^{15}\text{N}$ -labeled ammonium sulfate for the  $^1\text{H}$  and  $^{15}\text{N}$  channels and natural abundance adamantane for the  $^{13}\text{C}$  channel. The lossy samples are a uniformly  $^{15}\text{N}$  labeled membrane protein in phospholipid bilayers [16] loaded to 9 mm long in a 5 mm OD sample tube (New Era Enterprises ([www.newera-spectro.com](http://www.newera-spectro.com))) and a 35% random fractional  $^{13}\text{C}$ -labeled sample of the membrane bound form of Pf1 coat protein [10], which is loaded to 11 mm long in a 5 mm OD sample tube. The data were measured at room temperature.

The number of strips in each shield and the copper area, which is the total area covered by the copper, strongly affect the probe Q and the tuning frequency. For lower frequency channels, the probe Q increases as the copper area decreases. For higher frequency channels, the more the number of strips will lower the turning frequency and improve the probe Q with the lossy samples. The measurements in Table 2 use strip-shields made with 32 copper strips and each the strip is 14/32 inch long by 1/128 inch wide. The insertion of the strip-shield modestly decreases the probe Q on all channels even with non-lossy samples. However, it dramatically reduces the impact of lossy samples on the Q, especially at  $^1\text{H}$  and  $^{13}\text{C}$  frequencies. For example, without the shield, the probe Q drops from 181 to 63 on the  $^1\text{H}$  channel and from 137 to 81 on the  $^{13}\text{C}$  channel. Even at the  $^{15}\text{N}$  frequency, the Q is reduced by about 10%. For comparison, with the shield in place, the probe Q is only reduced from 163 to 139 in the  $^1\text{H}$  channel and from 114 to 110 in  $^{13}\text{C}$  channel.

RF heating effects are proportional to the power absorbed by the lossy samples. And the power absorbed is inversely proportional to the difference in Q with and without the samples [3;7]. Thus, the better the probe power efficiency for the lossy samples, the less the RF heating. The RF heating effects were measured using the same protocol described previously [17]. The “NMR thermometer” sample consists of 20 mM  $\text{Na}_5[\text{TmDOTP}]$  and an additional 70 mM of NaCl so that its dielectric properties are similar to those of a “worst case” lossy sample. For calibration, we use another “NMR thermometer”, ethylene glycol, where  $^1\text{H}$  chemical shift difference between the -OH and - $\text{CH}_2$  depends only on the temperature. We obtained two sets of data, one with the chemical shift difference of ethylene glycol as a function of temperature, and another with the  $^1\text{H}$  chemical shift of the H6 resonance of  $\text{Na}_5[\text{TmDOTP}]$  as a function of temperature.

The RF-induced heating data for all three channels are summarized in Figure 6, where the sample temperature is plotted as a function of the average RF field deposition, calculated as the product of square of  $B_1$  and the duty cycle factor.  $B_1$  of the  $^1\text{H}$  channel is measured directly using the NMR thermometer sample and is listed in Table 2.  $B_1$  of the  $^{13}\text{C}$  and  $^{15}\text{N}$  channel are estimated based on the Q of probes loaded with NMR thermometer sample presented in Table 2 and the linear relationship between the probe Q and the probe power efficiency. The power levels used in this study are 68 watts, 93 watts, and 375 watts for the  $^1\text{H}$ ,  $^{13}\text{C}$ , and  $^{15}\text{N}$  channels, respectively. The duty cycle factor is the ratio of the time that the RF irradiation is

on to the total duration of the pulse sequence. The sample is irradiated with an 8-minute pulse train with 1-second cycle time of various pulse lengths in order to establish thermal equilibrium. Immediately after the 8-minute irradiation, the  $^1\text{H}$  signals are signal averaged 100 times in 2 seconds. Sample heating during the signal averaging is ignored because of the low duty cycle irradiation during this period. The results of six sets of experiments are summarized in the Figure; they corresponding to the performance of the  $^1\text{H}$ ,  $^{13}\text{C}$ , and  $^{15}\text{N}$  channels with and without the strip-shield present. The slope represents the temperature rise (in  $^{\circ}\text{C}$ ) per square alternating magnetic field (in  $\text{kHz}^2$ ) generated. Without the shield, the slopes are 4.0, 1.81, and 1.01 ( $^{\circ}\text{C}/\text{kHz}^2$ ) for  $^1\text{H}$ ,  $^{13}\text{C}$ , and  $^{15}\text{N}$  channels, respectively, compared to 0.78, 0.27, and 1.24 ( $^{\circ}\text{C}/\text{kHz}^2$ ) with the shield present. For the  $^1\text{H}$  and  $^{13}\text{C}$  channels, the RF heating effects are improved by 5 and 7 fold, respectively. The RF-induced heating is 23% worse with the strip-shield at  $^{15}\text{N}$  channel even though the probe Q is essentially the same for non-lossy and lossy samples. This behavior is somewhat unexpected in the context of earlier RF heating analysis [7]. One explanation is the RF power dissipation by the sample coil due to resistance heating up any sample, lossy or non-lossy and with extra contribution from resistance heating of the copper in the strip-shield. Both effects could potentially be reduced using higher flow-rate cooling gas over the sample. This same effect on the  $^{15}\text{N}$  channel has been observed in another probe at 700 MHz.

The strip-shield probes are now in routine use for a variety of applications. Figure 7A is a  $^{15}\text{N}$  NMR spectrum of the uniformly  $^{15}\text{N}$ -labeled p7 protein in magnetically aligned phospholipid bilayers ( $q = 3.2$  bicelles). The spectrum was obtained from a single-contact cross-polarization experiment that was signal averaged for 4096 scans with 5 ms acquisition time and 7 s recycle delay. The  $B_1$  of both channels was set to 50 kHz. Figure 7B and 7C present  $^{13}\text{C}$  NMR spectra of the membrane-bound form of  $^{13}\text{C}$ -labeled Pf1 coat protein (7B) and a blank bicelle sample (7C). Both of these cross-polarization spectra resulted from signal averaging 2048 scans with 10 ms acquisition time and 5 s recycle delay. The  $B_1$  on both channels was set to 50 kHz. All three spectra are taken with MOIST [18] cross-polarization transfer and SPINAL16 [19] decoupling during acquisition. The spectra are zero-filled to 1024 points with 20 Hz line broadening applied prior to Fourier transformation.

## Discussion

A strip-shield coil liner, consisting of copper strips and PTFE insulator, inserted between a high inductance solenoid coil and the sample significantly ameliorates the effects of lossy samples on the performance of probes used for solid-state NMR at high fields. The probe efficiency is improved and the RF heating effect is reduced not only for the high frequency  $^1\text{H}$  channel but also for the  $^{13}\text{C}$  channel.

For probes that are designed only for non-lossy samples, introducing a strip-shield into the coil reduces the Q and the filling factor and should be avoided. The PTFE dielectric we used in the strip-shield generates  $^{13}\text{C}$  and  $^{19}\text{F}$  background signal. For direct  $^{13}\text{C}$  detection, the background signals are usually broad and are not in the region of aliphatic and carboxyl carbon, and are mostly filtered out with standard cross-polarization transfer technique. In order to remove  $^{19}\text{F}$  background signals, other dielectric material should be used. Concerns about the ability to shim the probe for high-resolution spectra turned out to be unfounded. Using the minimal set of shims, the  $\text{H}_2\text{O}$  line width to less than 0.1 ppm could be obtained with or without the shield present.

Compared to probes using inner solenoid coil as part of the cross-coil design [7;20], the strip-shield improves the probe efficiency for the  $^1\text{H}$  channel due to its better filling factor and  $^{13}\text{C}$  channel due to its better RF shielding. The tradeoff is about 10% lower probe efficiency at  $^{15}\text{N}$  channel due to lower coil quality factor and lower filling factor. In contrast, the lossy

samples reduce the probe power efficiency by 10% without the shield even at  $^{15}\text{N}$  frequency. Whether to use the strip-shield coil should be determined by the resonance frequency, how lossy is the sample, and the inductance of the solenoid coil. At medium frequencies such as  $^{13}\text{C}$  channel, improving the coil quality factor compensates the loss in filling factor. On the other hand, reducing the RF heating of samples is important since RF heating is not uniform across the sample volume, and substantial temperature gradient will broaden the spectral lines, reduce the signal-to-noise ratio, and possibly damage the samples. The strip-shield reduce the RF heating by 5 to 7 fold at both  $^1\text{H}$  frequency and  $^{13}\text{C}$  frequency. The reduction in RF heating is sufficient to enable the implementation of fast recycle experiments [21]. At  $^{15}\text{N}$  frequency, the performance of the strip-shield coils is acceptable but is not optimal compared to traditional solenoid coils.

The benefits of the strip-shield are most pronounced at the  $^1\text{H}$  and  $^{13}\text{C}$  resonance frequencies in high magnetic fields. Double-resonance  $^1\text{H}$ - $^{13}\text{C}$  probes that use strip-shield coil perform exceptionally well compared to other coil designs for lossy samples. Similar benefits are obtained in probes with  $^1\text{H}/^{13}\text{C}/^{15}\text{N}$  triple-tuned probes.

## Acknowledgments

We thank Lena Jairam for help with sample preparation and Werner Maas of Bruker BioSpin for the generous gift of the “gold fingers” used in the probe construction. This research was supported by grants from the National Institutes of Health, and was performed at the Biotechnology Resource for NMR Molecular Imaging of Proteins, which is supported by grant P41EB002031.

## References

1. Krahn A, Priller U, Emsley L, Engelke F. Resonator with reduced sample heating and increased homogeneity for solid-state NMR. *Journal of Magnetic Resonance* 2008;191:78–92. [PubMed: 18187352]
2. Li C, Mo Y, Hu J, Chekmenev E, Tian C, Fu R, Gor'kov P, Brey W, Cross TA. Analysis of RF heating and sample stability in aligned static solid-state NMR spectroscopy. *Journal of Magnetic Resonance* 2006;180:51–57. [PubMed: 16483809]
3. Doty FD, Kulkarni J, Turner C, Entzminger G, Bielecki A. Using a cross-coil to reduce RF heating by an order of magnitude in triple-resonance multinuclear MAS at high fields. *Journal of Magnetic Resonance* 2006;182:239–253. [PubMed: 16860580]
4. Paulson EK, Martin RW, Zilm KW. Cross polarization radio frequency field homogeneity, and circuit balancing in high field solid state NMR probes. *Journal of Magnetic Resonance* 2004;171:314–323. [PubMed: 15546758]
5. Stringer JA, Bronnimann CE, Mullen CG, Zhou DH, Stellfox SA, Li Y, Williams EH, Rienstra CM. Reduction of RF-induced sample heating with a scroll coil resonator structure for solid-state NMR probes. *J Magn Reson* 2005;173:40–48. [PubMed: 15705511]
6. Alderman DW, Grant DM. An efficient decoupler coil design which reduces heating in conductive samples in superconducting spectrometers. *Journal of Magnetic Resonance* (1969) 1979;36:447–451.
7. Gor'kov PL, Chekmenev EY, Li CG, Cotten M, Buffy JJ, Traaseth NJ, Veglia G, Brey WW. Using low-E resonators to reduce RF heating in biological samples for static solid-state NMR up to 900 MHz. *Journal of Magnetic Resonance* 2007;185:77–93. [PubMed: 17174130]
8. Dillmann B, Elbayed K, Zeiger H, Weingartner M-C, Piotto M, Engelke F. A novel low-E field coil to minimize heating of biological samples in solid-state multinuclear NMR experiments. *Journal of Magnetic Resonance* 2007;187:10–18. [PubMed: 17448715]
9. Zhang QW, Zhang H, Lakshmi KV, Lee DK, Bradley CH, Wittebort RJ. Double and Triple Resonance Circuits for High-Frequency Probes. *Journal of Magnetic Resonance* 1998;132:167–171.
10. Sinha N, Filipp FV, Jairam L, Park SH, Bradley J, Opella SJ. Tailoring  $^{13}\text{C}$  labeling for triple-resonance solid-state NMR experiments on aligned samples of proteins. *Magnetic Resonance in Chemistry* 2007;45:s107–s115. [PubMed: 18157808]



11. De Angelis AA, Opella SJ. Bicelle samples for solid-state NMR of membrane proteins. *Nature Protocols* 2007;2:2332–2338.
12. Idziak S, Haeberlen U. Design and construction of a high homogeneity rf coil for solid-state multiple-pulse NMR. *Journal of Magnetic Resonance* 1982;50:281–288.
13. Cross VR, Hester RK, Waugh JS. Single coil probe with transmission-line tuning for nuclear magnetic double-resonance. *Review of Scientific Instruments* 1976;47:1486–1488.
14. Hoult DI. The principle of reciprocity in signal strength calculations†-†A mathematical guide. *Concepts in Magnetic Resonance* 2000;12:173–187.
15. Clark WG, McNeil JA. Single Coil Series Resonant Circuit for Pulsed Nuclear Resonance. *Review of Scientific Instruments* 1973;44:844–851.
16. De Angelis AA, Howell SC, Nevzorov AA, Opella SJ. Structure Determination of a Membrane Protein with Two Trans-membrane Helices in Aligned Phospholipid Bicelles by Solid-State NMR Spectroscopy. *Journal of the American Chemical Society* 2006;128:12256–12267. [PubMed: 16967977]
17. Grant CV, Sit S-L, De Angelis AA, Khuong KS, Wu CH, Plesniak LA, Opella SJ. An efficient  $^1\text{H}/^31\text{P}$  double-resonance solid-state NMR probe that utilizes a scroll coil. *Journal of Magnetic Resonance* 2007;188:279–284. [PubMed: 17719813]
18. Levitt MH, Suter D, Ernst RR. Spin Dynamics and thermodynamics in solid-state NMR cross polarization. *Journal of Chemical Physics* 1986;84:4243–4255.
19. Fung BM, Khitrin AK, Ermolaev K. An improved broadband decoupling sequence for liquid crystals and solids. *Journal of Magnetic Resonance* 2000;142:97–101. [PubMed: 10617439]
20. Grant CV, Yang Y, Glibowicka M, Wu CH, Grant SH, Deber C, Opella SJ. A modified Alderman-Grant coil makes possible an efficient cross-coil probe for high field solid-state NMR of lossy biological samples. 2009
21. Wickramasinghe NP, Parthasarathy S, Jones CR, Bhardwaj C, Long F, Kotecha M, Mehboob S, Fung LWM, Past J, Samoson A, Ishii Y. Nanomole-scale protein solid-state NMR by breaking intrinsic  $^1\text{H}$   $T_1$  boundaries. *Nat Meth* 2009;6:215–218.

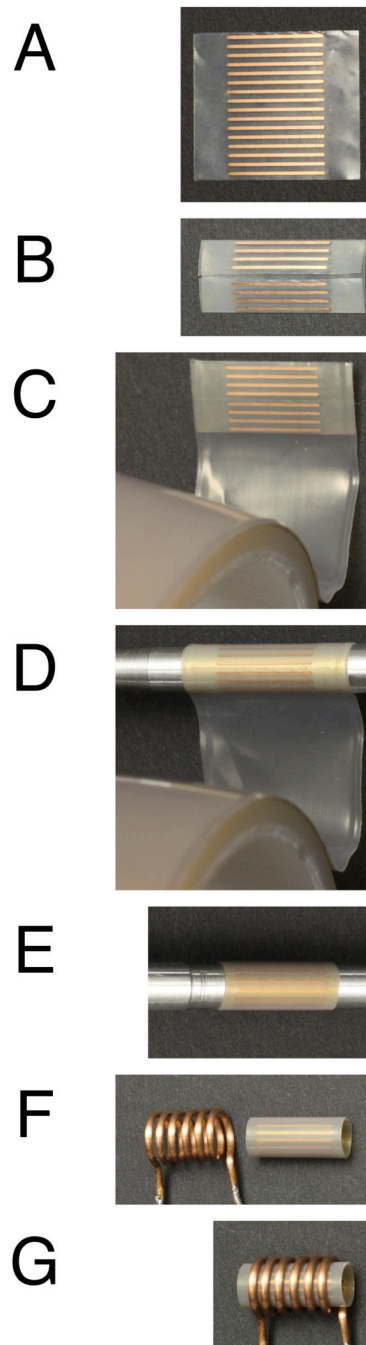


**Figure 1.** Constructions of a strip-shield. (A) One strip-shield is cut from the larger PTFE sheet. (B) With the copper on the outside, the sheet is rolled to form a cylinder. (C) PTFE tape is applied to connect the ends. (D) The rolled sheet is placed on a 5 mm OD cylinder, and wrapped with two layers of PTFE tape. (E) Excess PTFE is cut off from both ends. (F) The strip-shield is inserted into a 5.6 mm ID solenoid coil. (G) The completed strip-shield/coil assembly.

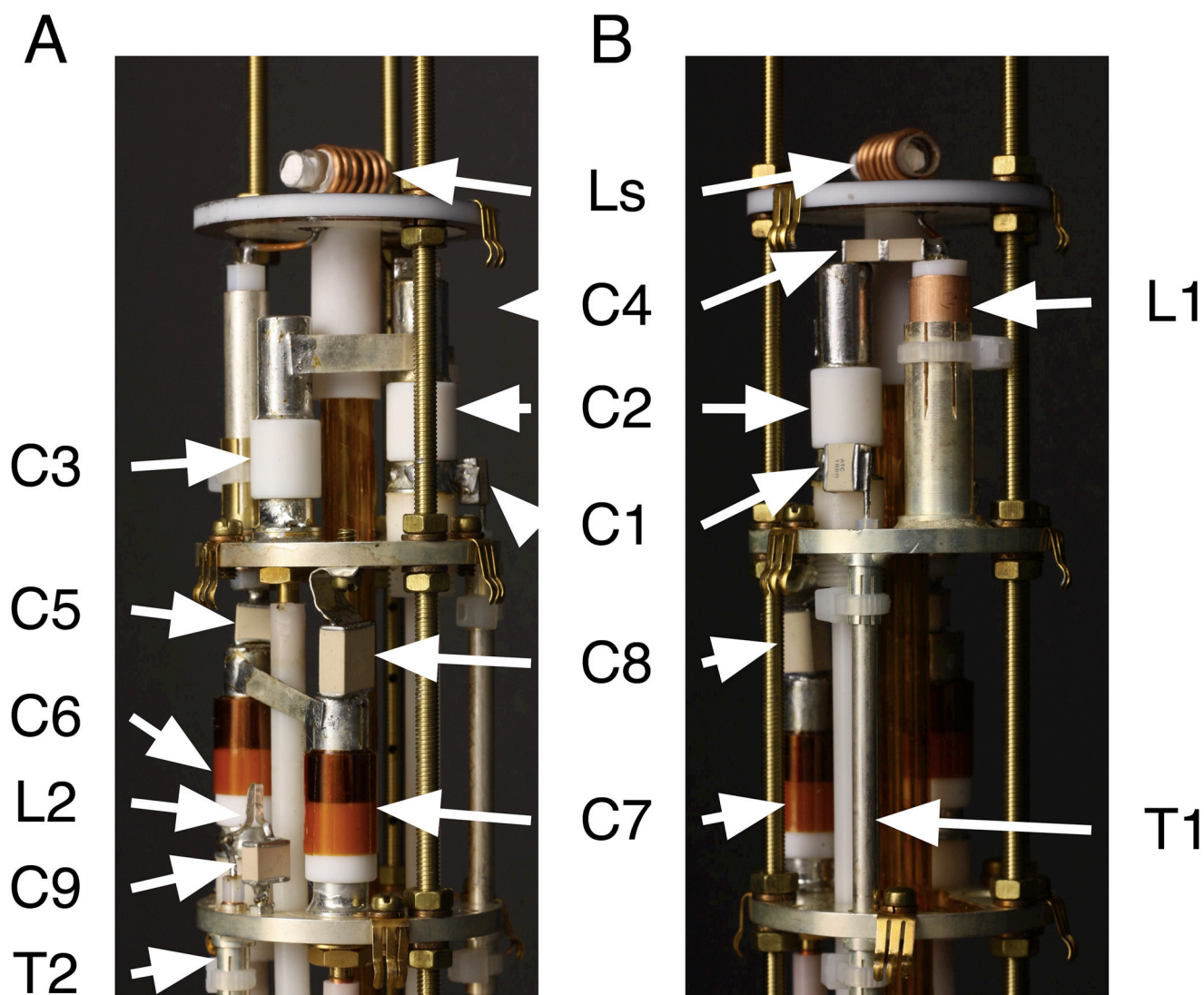


**Figure 2.** Photographs of a  $^1\text{H}/^{15}\text{N}$  double-resonance probe. (A) and (B) differ by 90o rotation. The inductors and capacitors are designated as in Figure 3A and their values are listed in Table 1.

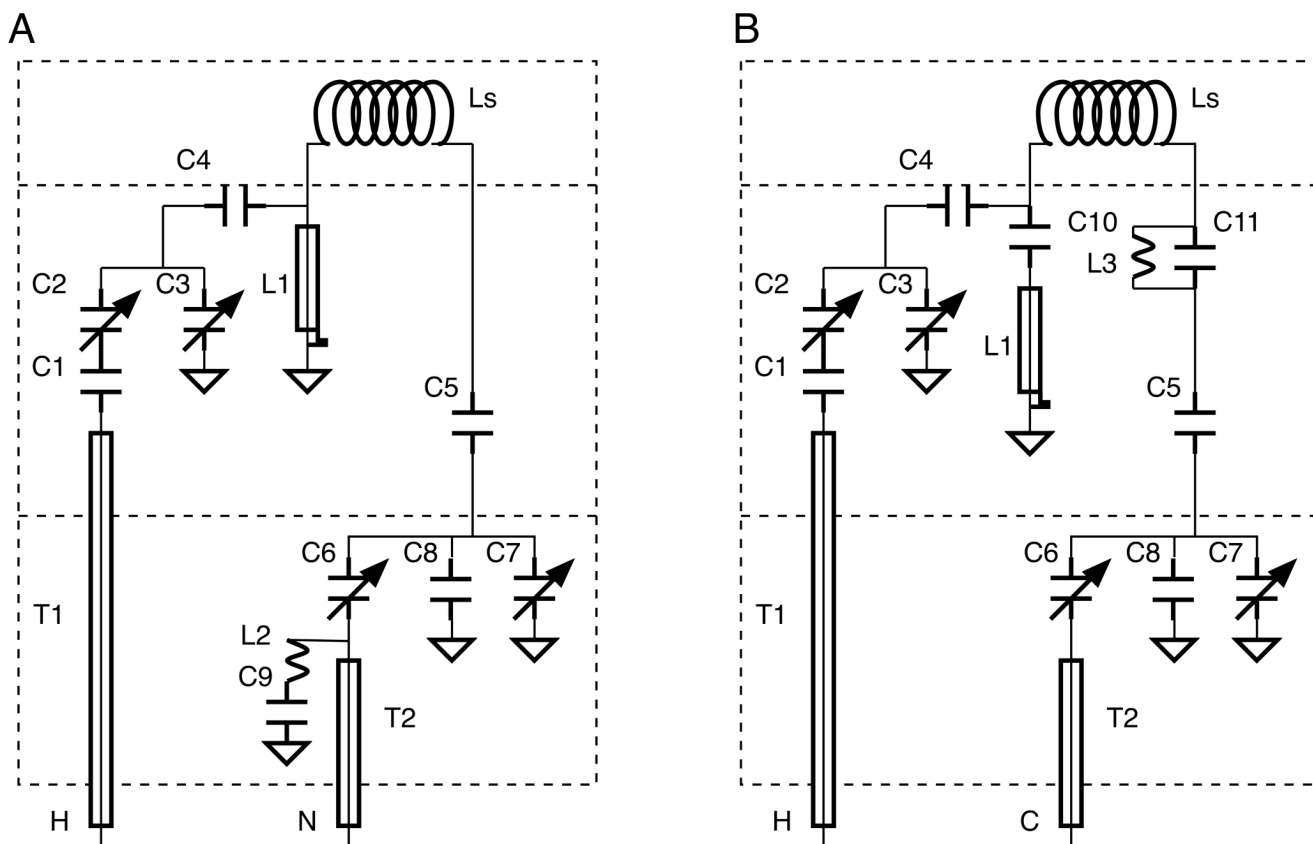


**Figure 3.** (A) Circuit diagram of the  $^1\text{H}/^{15}\text{N}$  double-resonance probe. (B) Circuit diagram of the  $^1\text{H}/^{13}\text{C}$  double-resonance probe.

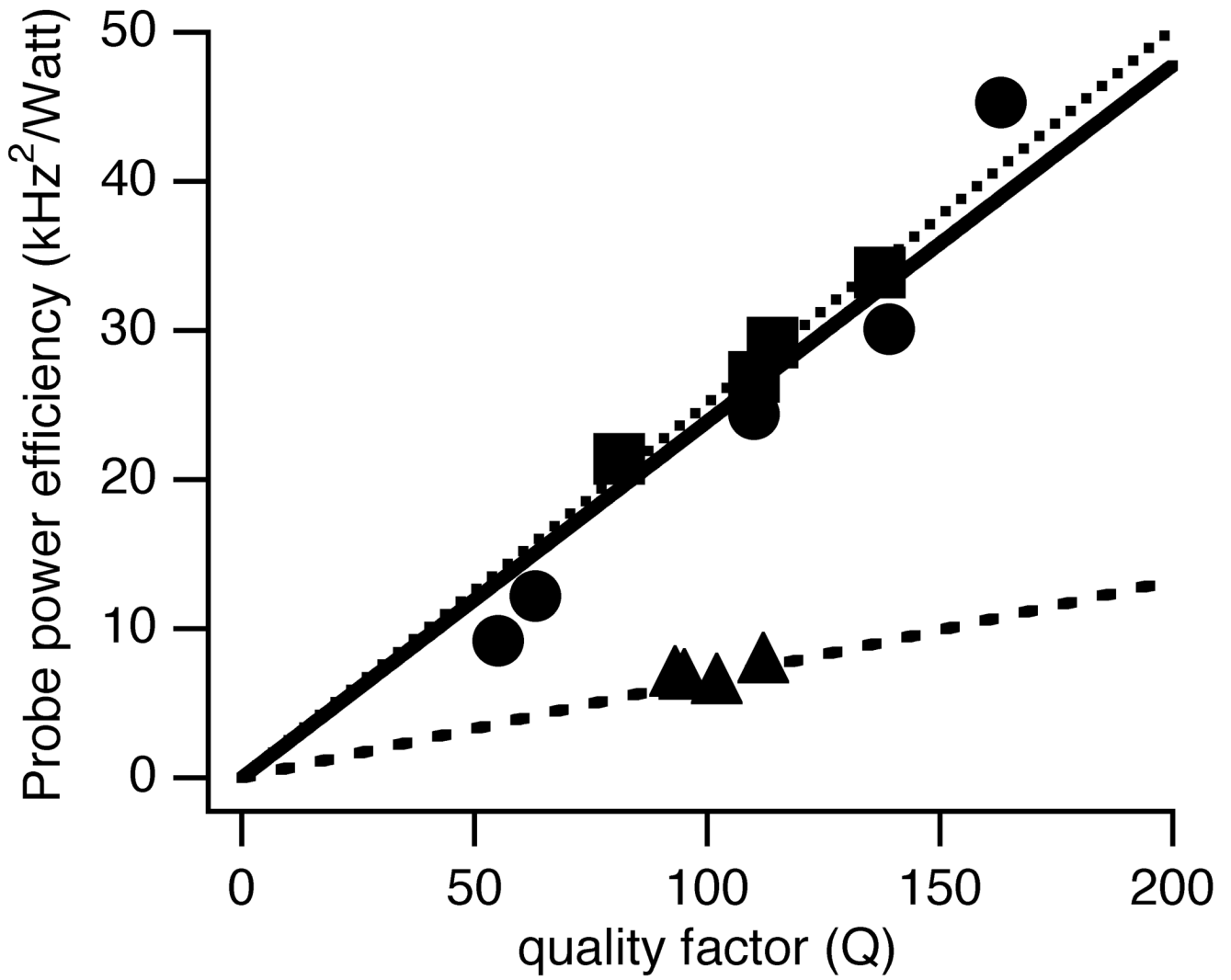


**Figure 4.** Plots of probe power efficiency vs. the quality factor of the circuit. Circle: <sup>1</sup>H channel; Squares: <sup>13</sup>C channel; Triangles: <sup>15</sup>N channel.

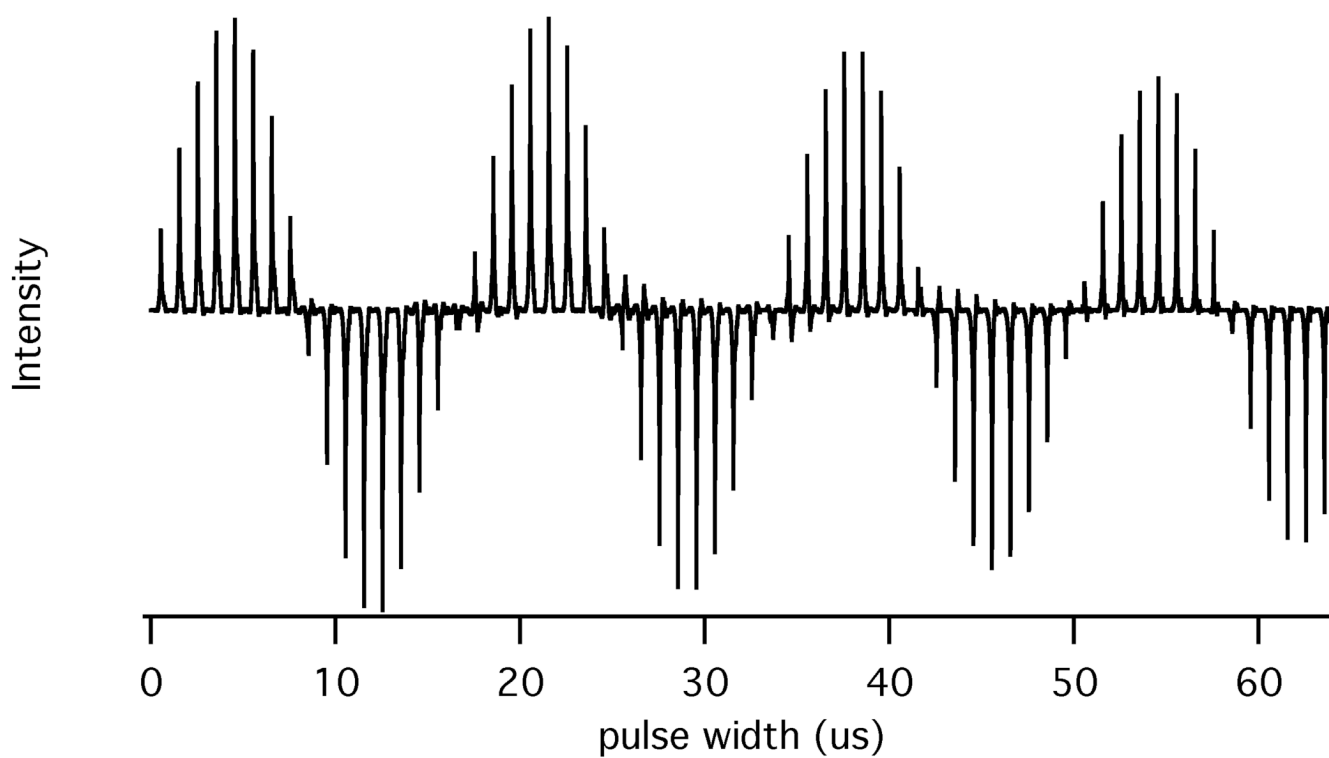


**Figure 5.**

$^1\text{H}$  nutation plot at 800 MHz for the water resonance in a typical bicelle sample in a 9 mm long and 5 mm OD sample tube. The nutation plot is obtained by measuring the resonance intensities following direct excitation with pulses of various durations.

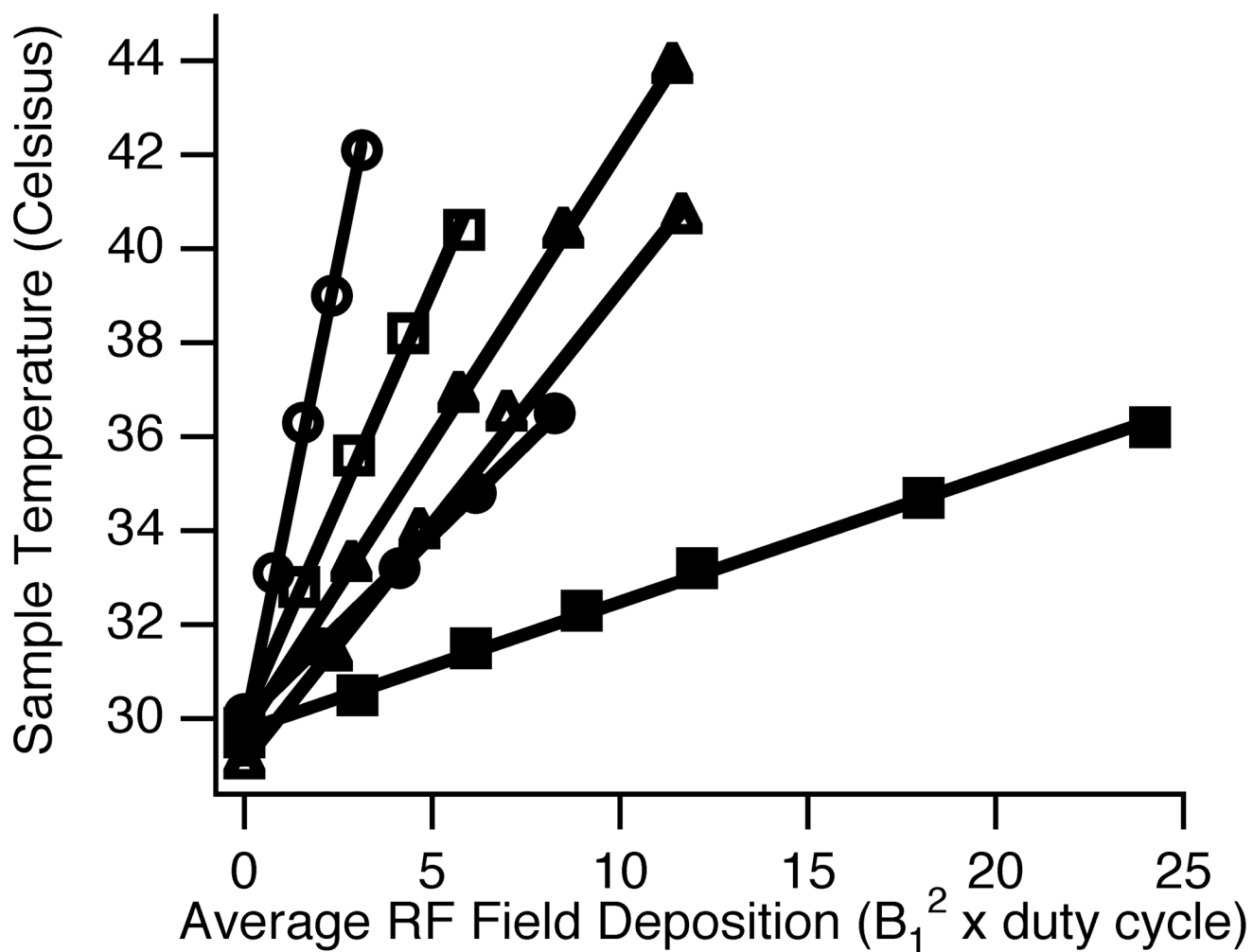


**Figure 6.** Plots of measured sample temperature vs. RF Power Deposition. Open symbols: without shield; Filled symbols: with shield; Circles:  $^1\text{H}$  channel; Squares:  $^{13}\text{C}$  channel; Triangles:  $^{15}\text{N}$  channel.

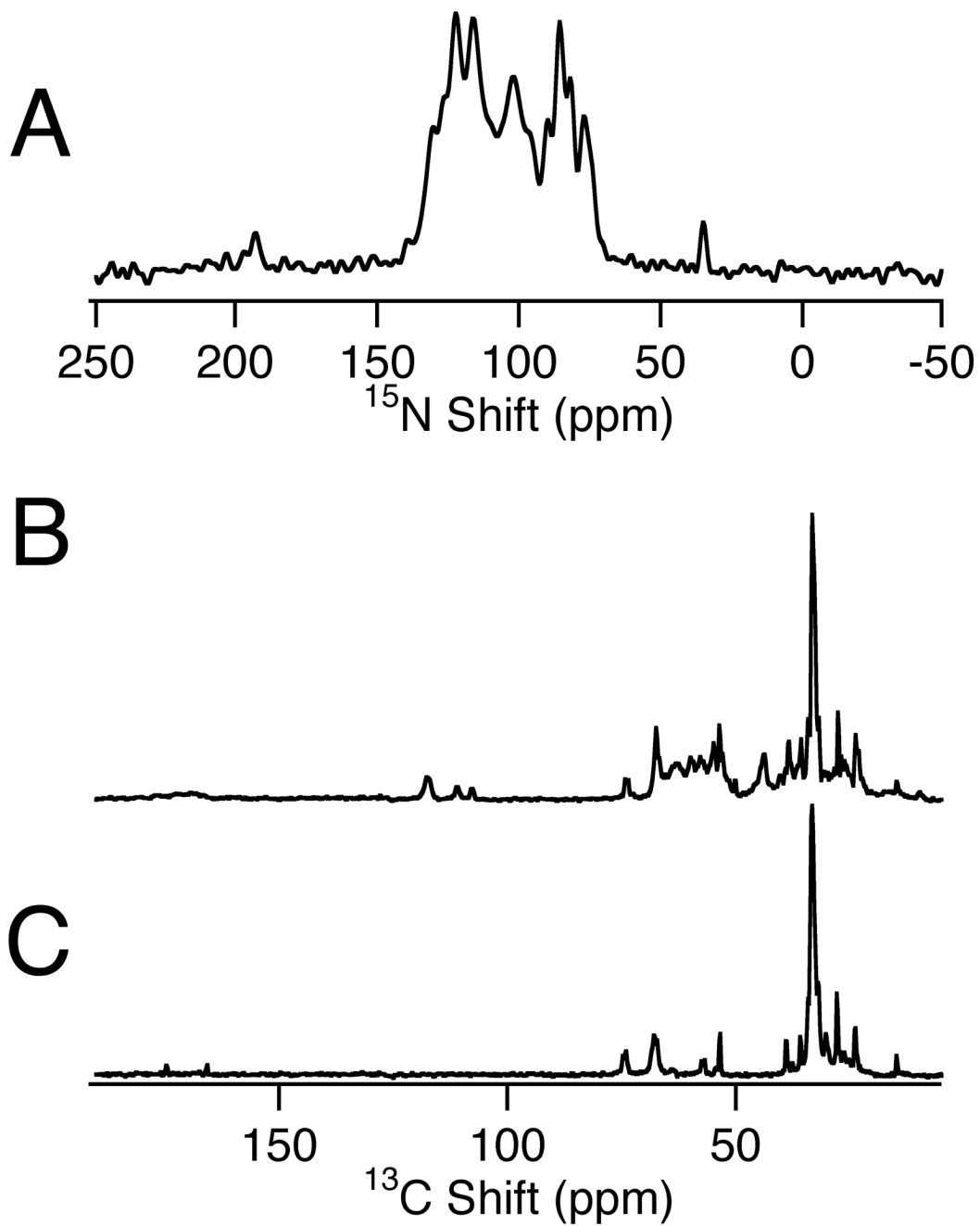


**Figure 7.**

One-dimensional spectra of various magnetically aligned bicelle samples. (A)  $^{15}\text{N}$  NMR spectrum of uniformly  $^{15}\text{N}$  labeled p7 protein from HCV in magnetically aligned bicelles. (B)  $^{13}\text{C}$  NMR spectrum of partially  $^{13}\text{C}$  labeled Pf1 coat protein in magnetically aligned bicelles. (C)  $^{13}\text{C}$  NMR spectrum of bicelles without protein; the comparison of (B) and (C) enables the protein resonances to be distinguished.



**Table 1**

List of capacitance values of the two 800 MHz double-resonance probes. The component symbols are designated in Figure 3.

Component	<sup>1</sup> H- <sup>15</sup> N	<sup>1</sup> H- <sup>13</sup> C
C1	1 pf	2.2 pf
C4	0.6 pf	0.6 pf
C5	27 pf	56 pf
C8	39 pf	-
C9	3.9 pf	-
C10	-	5.6 pf
C11	-	5.6 pf
L1	30 mm	35 mm

**Table 2**

Performance data. Q is the probe quality factor.  $\eta$  is the probe power efficiency and is defined as the square of nutation frequency ( $B_1$ ), in kHz, divided by the power.

		<b>1H (801 MHz)</b>	<b>13C (201 MHz)</b>	<b>15N (81 MHz)</b>
without shield	Q non-lossy	181	137	112
	Q lossy	63	81	102
	$\eta$ (kHz <sup>2</sup> /Watt) non-lossy		33.9	7.5
	$\eta$ (kHz <sup>2</sup> /Watt) lossy	12.2	21.4	6.1
	Q 70 mM NaCl	55	50	94
	$\eta$ (kHz <sup>2</sup> /Watt) 70 mM NaCl	9.2		
with shield	Q non-lossy	163	114	95
	Q lossy	139	110	93
	$\eta$ (kHz <sup>2</sup> /Watt) non-lossy	45.3	29.2	6.4
	$\eta$ (kHz <sup>2</sup> /Watt) lossy	30.1	26.9	6.6
	Q 70 mM NaCl	110	103	92
	$\eta$ (kHz <sup>2</sup> /Watt) 70 mM NaCl	24.4		